Variations in late syn-rift melt alignment inferred from shear-wave splitting in crustal earthquakes beneath the Ethiopian rift

Derek Keir,[1] J-M. Kendall,[2,3] C. J. Ebinger,[1] and G. W. Stuart[2]

Received 21 July 2005; revised 12 October 2005; accepted 25 October 2005; published 8 December 2005.

[1] The northern Main Ethiopian rift (MER) marks the transition from continental rifting to incipient seafloor spreading. We constrain anisotropy of the upper-crust in the MER and its uplifted rift flanks using shear-wave splitting from 24 earthquakes located beneath 18 broadband stations. Along the axis of the MER the fast polarization direction is oriented between ~N and ~NNE, parallel to Quaternary-Recent faults, aligned cones and maximum horizontal stress. Delay times are highest (0.24 s) where independent seismic studies show evidence of shallow partial melt. We attribute anisotropy along the rift axis to aligned melt-filled micro-cracks and dikes. At stations flanking the rift, the fast polarization direction is oriented ~NE and delay-times are smaller (0.04–0.14 s). The lower amount of anisotropy is consistent with reduced melt away from the rift axis. These results show melt-induced anisotropy persists into the crust, and magma injection localizes and accommodates strain just prior to continental break-up. **Citation:** Keir, D., J-M. Kendall, C. J. Ebinger, and G. W. Stuart (2005), Variations in late syn-rift melt alignment inferred from shear-wave splitting in crustal earthquakes beneath the Ethiopian rift, *Geophys. Res. Lett.*, *32*, L23308, doi:10.1029/2005GL024150.

1. Introduction

[2] Strain localizes as rifting proceeds to continental breakup, but the partitioning of strain between mechanical failure and magma injection remains controversial. The volcanically active northern Main Ethiopian rift (MER) is transitional between continental and incipient oceanic rifting [e.g., *Ebinger and Casey*, 2001], affording the opportunity to actively observe rift processes just prior to break-up.

[3] The Miocene-Recent MER constitutes the northern part of the East African rift system and forms the youngest arm of the Afar triple junction, which developed in the Eocene-Oligocene flood basalt province (Figure 1, inset). The MER is bounded by NE-trending Miocene border faults. Since Quaternary times extensional strain is localized in <20 km-wide right stepping en-echelon magmatic segments which are zones of NNE-striking fissures, faults and aligned volcanic cones [*Bilham et al.*, 1999; *Ebinger and Casey*, 2001]. These magmatic segments are the locus of seismicity and magmatism (D. Keir et al., Strain accommodation by magmatism and faulting as rifting proceeds to breakup: Seismicity of the northern Ethiopian rift, submitted to *Journal of Geophysical Research*, 2005, hereinafter referred to as Keir et al., submitted manuscript, 2005) (Figure 1). The current extension direction is ~N105°E [*Wolfenden et al.*, 2004; Keir et al., submitted manuscript, 2005].

[4] Anisotropy provides further constraints on style of rifting and breakup. SKS-splitting dominantly reflects upper-mantle anisotropy, and measurements in the MER show a rift-parallel (~NNE) fast anisotropic orientation that parallels the aligned eruptive centers, fissures and active faults. The magnitude of splitting and cross-rift variation in the orientation of the fast S-wave were used to propose that partial melt beneath the MER rises through melt-filled cracks that penetrate the thinned lithosphere [*Kendall et al.*, 2005a]. Sv and Sh velocity models determined from inversion of surface-wave dispersion curves show faster Sv velocities than Sh velocities below 20 km along the rift axis. The results are consistent with anisotropy at 20–75 km depth due to oriented melt-filled pockets [*Kendall et al.*, 2005b]. *Bastow et al.* [2005] show, by comparing P-and S-wave relative arrival-time data, that upper mantle low velocity anomalies beneath the MER are likely due to high-temperatures and partial melt.

[5] Anisotropy of the shallow crust is commonly attributed to micro-cracks vertically-oriented parallel to the direction of maximum horizontal stress [e.g., *Crampin*, 1994]. For example, crustal shear-wave splitting measurements in rift zones at the Mid-Atlantic ridge and in Iceland show fast-polarization directions sub-parallel to the maximum horizontal stress. These patterns are attributed to aligned parallel cracks and fractures in the uppermost 3–5 km of the crust [e.g., *Barclay and Toomey*, 2003; *Evans et al.*, 1996; *Menke et al.*, 1994]. S-wave anisotropy has also been attributed to vertical micro-cracks throughout the crust in which case S-wave splitting is accrued along the whole ray-path [e.g., *Volti and Crampin*, 2003]. Fast-polarization directions at active volcanoes are usually parallel to dikes and the maximum horizontal stress, with 90° polarization flips observed prior to volcanic eruption due to increased pore pressure leading to changes in crack orientation [*Miller and Savage*, 2001]. Crustal anisotropy has also been linked to other rock fabrics such as vertically dipping foliation of metamorphic basement [e.g., *do Nascimento et al.*, 2004]. We use measurements of S-wave splitting from local earthquakes to study crustal anisotropy in the MER. We compare our results to independent studies and use this information to evaluate mechanisms of deformation preceding continental break-up.

2. Data and Methodology

[6] From October 2001 to January 2003, seismicity was recorded by 29 broadband instruments that covered a

[1]Department of Geology, Royal Holloway University of London, Egham, UK.
[2]School of Earth and Environment, University of Leeds, Leeds, UK.
[3]Now at Department of Earth Sciences, University of Bristol, Bristol, UK.

0094-8276/05/2005GL024150$05.00

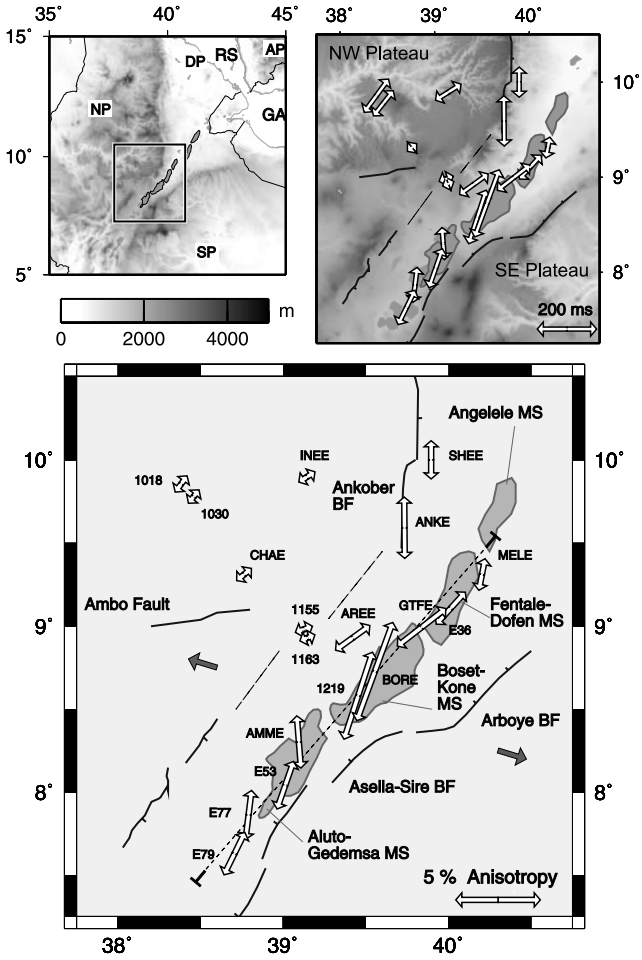

Figure 1. Crustal anisotropy measurements at 18 broadband stations in Ethiopia. White arrows show the polarization of the fast S-wave (ϕ) and arrow length is scaled by % anisotropy. Solid black lines with dip ticks are Miocene border faults (BF) and dashed lines are monoclines. Quaternary magmatic segments (MS) are shaded grey. Dark arrows show the extension direction and orientation of the minimum horizontal stress (Keir et al., submitted manuscript, 2005). The position of the along-axis profile for Figures 2b and 2d is shown by the black line. Top left inset: Topographic map of the MER, adjacent plateau and Afar depression. NP: Nubia Plate, SP: Somali Plate, DP: Danakil Plate, AP: Arabian Plate, RS: Red Sea, GA: Gulf of Aden. Top right inset: White arrows show polarization of fast S-wave and arrow length is scaled by delay-time.

250 km × 350 km area of the MER and adjacent uplifted plateau [*Bastow et al.*, 2005]. A further 150 broadband instruments operated for the final 2-4 months of the experiment (Keir et al., submitted manuscript, 2005). Earthquakes were located using a 3-D velocity model determined from local earthquake tomography (Keir et al., submitted manuscript, 2005). 75% of seismicity occurred in the Fentale-Dofen magmatic segment and at the intersection of the MER and Red Sea rift (Keir et al., submitted manuscript, 2005). Due to this severe spatial clustering of earthquakes, S-wave splitting measurements could only be made at ~10% of available seismic stations (Figure 1). 24 earthquakes located beneath 18 stations provided 26 three-component seismograms where the S-wave incident-angle is within the shear-wave window (SWW). The SWW is the vertical cone bound by $\sin^{-1}$ (Vs/Vp) where S-wave particle motions are not disturbed by S-P conversions at the free surface [*Booth and Crampin*, 1985]. We use a Vp/Vs of 1.75, calculated from P- and S-wave travel-times from earthquakes in the MER, which corresponds to a SWW that is a cone within 35° of the vertical.

[7] The polarization direction of the fast S-wave (ϕ) and the time delay between the fast and slow S-waves (δt) is determined using the method of *Silver and Chan* [1991], adapted for application to micro-earthquakes. In an isotropic radially stratified crust, near vertically impinging S-waves should exhibit linear particle motion. This phase is split into orthogonally polarized fast and slow S-waves when it travels through an anisotropic medium and this splitting produces an elliptical particle motion. To remove the effects of the anisotropy we rotate the horizontal components by ϕ and shift their relative positions by δt, thereby linearizing the particle motion (Figure S1, auxiliary material[1]). To estimate the splitting we search for the correction parameters that best linearize the S-wave motion. An F-test is performed to assess the uniqueness of the estimated splitting parameters and thereby produce an error estimate [*Silver*, 1996]. The splitting parameters are well constrained. We use a cut off error criteria of ± 0.03 s for δt and 9° for ϕ (Table S1, auxiliary material).

3. Results

[8] S-wave splitting measurements from local earthquakes near the MER show large spatial variation in both ϕ and δt (Figure 1). At stations on the NW plateau ϕ varies between 36° and 70°. δt varies between 0.04 s and 0.14 s for earthquakes that occurred at depths of 12–20 km and δt increases linearly with increased ray-path distance (Figure 2), showing that the crust is anisotropic to at least 20 km depth. This equates to fairly uniform anisotropy of 1.1 % on average, if splitting is assumed to be accrued over the full ray-path length (Figures 1 and 2).

[9] Along the Ankober fault system ϕ is oriented ~N, parallel to seismically active faults (Figure S1). δt is 0.1–0.16 s, equivalent to 2.2–3.6 % S-wave anisotropy.

[10] At stations along the rift axis ϕ is mostly oriented ~N to NNE (Figure 1). Delay times are 0.06–0.24 s for earthquakes that are 6–9 km deep, equating to 3–6.2 % anisotropy (Figure 2). The largest values of δt (0.19–0.24 s, anisotropy of 5.4–6.2 %) are recorded at stations 1219 and BORE, both in the Quaternary Boset-Kone magmatic segment (Figures 1 and 2).

4. Discussion

[11] Near-vertically propagating S-waves from local earthquakes near the MER show clear evidence of S-wave splitting. The anisotropy is thus most likely due to foliations, cracks or inclusions aligned by regional and local stresses in the crust. The magnitude and orientation of the shear-wave splitting varies dramatically across the EAGLE network, suggesting a heterogeneous stress field or varia-

[1]Auxiliary material is available at ftp://ftp.agu.org/apend/gl/2005GL024150.

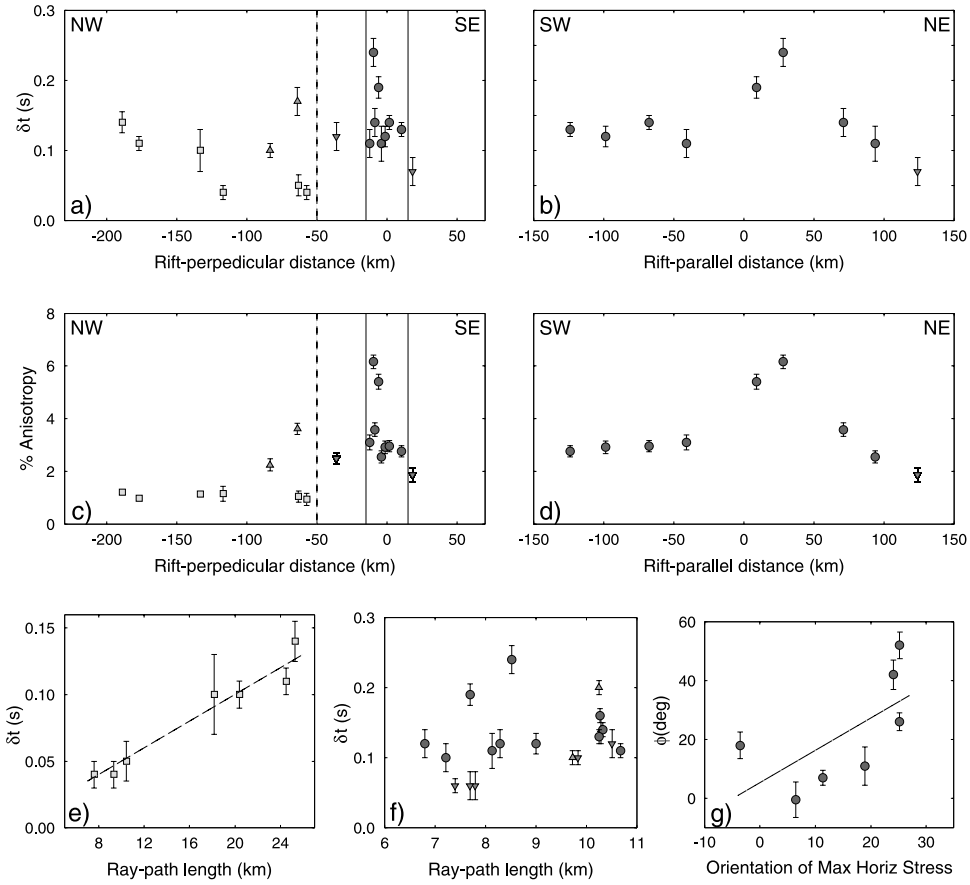

Figure 2. (a) Rift-perpendicular profile of station averaged delay time (δt) versus distance from the rift axis. The two solid lines shows the position of magmatic segments and the dashed line shows the approximate position of the western boundary of the rift valley. (b) Rift-parallel profile of station averaged δt at stations within 20 km of the along rift-axis line on Figure 1. (c) Rift perpendicular profile of % anisotropy versus distance from the rift axis. (d) Rift-parallel profile of % anisotropy versus distance along the rift valley. (e) Individual measurements of δt versus S-wave ray-path length at stations on the western Ethiopian plateau. The dashed line is the best straight line fit to the data. (f) Individual measurements of δt versus ray-path length at stations in the rift valley. (g) φ against the average orientation of maximum horizontal stress axes of focal mechanisms within 25 km of the splitting measurement. The dashed line is the best straight line fit to the data. The symbols are: white squares = plateau stations; grey triangles = stations at the Ankober fault; inverted triangles = stations in the MER but outside magmatic segments; dark grey circles = stations in magmatic segments.

tions in the underlying cause of anisotropy. We calibrate our results with independent geological and seismic studies in the MER.

[12] Stations along the rift axis show relatively large amounts of splitting despite shallower earthquake depths (6–9 km). Up to 0.24 s of splitting is observed beneath Boset-Kone magmatic segment, which equates to over 6 % anisotropy. Stations within the rift valley but located outside magmatic segments show less splitting (e.g. MELE), but the average magnitude of splitting in the rift valley is still nearly 3%, much larger than beneath the NW plateau. The ~N to NNE orientation of φ in the magmatic segments is parallel to Quaternary faults and aligned volcanic cones. The along axis variation of φ correlates well with local changes in the strike of maximum horizontal stress axes from focal mechanisms of earthquakes within 25 km of splitting measurements (Figure 2) (Keir et al., submitted manuscript, 2005).

[13] The largest amounts of upper-crustal anisotropy are in the Quaternary magmatic segments where independent studies show evidence of pervasive dike intrusion and the presence of partial melt in shallow magma chambers. *Mackenzie et al.* [2005] and *Keranen et al.* [2004] interpret cooled mafic intrusions in the mid-crust beneath these magmatic segments using models derived from wide-angle refraction data and controlled source tomography respectively. The magnitude of splitting under Boset volcano is especially pronounced, where melt-related anomalies have been interpreted in magnetotelluric data [*Whaler and Hautot*, 2005]. The S-wave splitting observations are consistent with anisotropy due to vertically aligned magma intrusions or melt-filled cracks beneath the Quaternary magmatic segments, where the majority of strain is accommodated by dike injection (Keir et al., submitted manuscript, 2005).

[14] The deepest earthquakes lie beneath the largely unextended NW Ethiopian plateau, where we observe an increase in delay time with increased ray-path length using S-wave splitting measurements at different stations. These variations in delay-times can be explained by relatively uniform anisotropy that extends to at least 20 km depth; larger delay-times (0.1–0.14 s) at stations 1018, 1030 and INEE are caused by splitting accrued over longer ray-paths

(Figures 1 and 2). Alternatively, these patterns may be caused by lateral variations in anisotropy of the uppermost few kilometers with larger upper crustal anisotropy at stations 1018, 1030 and INEE. However, controlled source seismic images of underplating [*Mackenzie et al.*, 2005], mid-crustal conductive anomalies in MT data [*Whaler and Hautot*, 2005], and Quaternary eruptive centers as far north as Lake Tana all infer the presence of melt in the lower crust beneath the Ethiopian plateau. Given these independent observations, we interpret the data to show that melt induced anisotropy extends to at least 20 km subsurface. The amount of crustal anisotropy beneath the plateau is low (1.1%), consistent with melt decrease away from the rift axis. Splitting at stations on the plateau is oriented ~NE and may also indicate a contribution from pre-existing basement foliation or structural trends. Where exposed, Pan-African basement foliation and Proterozoic ophiolite belts predominantly strike ~N to ~NE [e.g., *Berhe*, 1990; *Kazmin et al.*, 1978]. These have been used to infer a NE-SW trending suture [*Berhe*, 1990] but due to limited basement outcrop their interpretation is controversial [*Church et al.*, 1991]. NE to ENE oriented basement structures are evident in regional drainage patterns along the Ambo fault, which has been reactivated in Miocene rifting [*Abebe et al.*, 1998]. Beneath the Ethiopian plateau the crustal anisotropy may be due to a combination of mechanisms associated with aligned melt, pre-existing basement foliation and structural trends.

[15] The patterns of shear-wave splitting observed in earthquakes beneath both the rift valley and nearby plateau are most simply explained by crustal anisotropy related to variable amounts of melt pocket alignment, with a higher degree of magma intrusion in the crust beneath the rift. Our study shows that melt-induced anisotropy at 20–75 km depth [*Bastow et al.*, 2005; *Kendall et al.*, 2005a, 2005b] continues into the uppermost crust, thereby penetrating the entire plate and facilitating continental breakup.

5. Conclusions

[16] Along the rift-axis the orientation of the fast S-wave is ~N to NNE, parallel to Quaternary to Recent faults, aligned cones and the current maximum horizontal stress axis. The largest amounts of upper crustal anisotropy are in the Quaternary magmatic segments, where the majority of strain is accommodated by magma injection; anisotropy is most likely caused by aligned melt-filled micro-cracks and dikes. The low amount of anisotropy beneath the Ethiopian plateau is consistent with melt decrease away from the rift axis. These results suggest the anisotropy is related to variable amounts of melt pocket alignment in the crust, with a higher degree of dike intrusion in a narrow zone of Quaternary magmatism. Melt-induced anisotropy extends from the base of the lithosphere to the upper crust, suggesting that magma injection helps localize and facilitate extension just prior to continental breakup.

[17] **Acknowledgments.** We thank SEIS-UK and A. Brisbourne for the use of instruments and assistance in the field. The support provided by A. Ayele and L. Asfaw of the Geophysical Observatory, Addis Ababa University is much appreciated. The input provided by E. Daly, I. Bastow, D. Cornwell, P. Maguire and K. Whaler is also gratefully acknowledged. We thank Stuart Crampin and the anonymous reviewer who helped improve this manuscript. This research was supported by NERC grant NER/A/S/2000/01004 and NERC studentship NER/S/A/2002/10547.

References

Abebe, T., F. Mazzarini, F. Innocenti, and P. Manetti (1998), The Yerer-Tullu Wellel volcanotectonic lineament: A transtensional structure in central Ethiopia and the associated magmatic activity, *J. Afr. Earth Sci.*, *26*(1), 135–150.

Barclay, A. H., and D. R. Toomey (2003), Shear wave splitting and crustal anisotropy at the Mid-Atlantic Ridge, 35°N, *J. Geophys. Res.*, *108*(B8), 2378, doi:10.1029/2001JB000918.

Bastow, I. D., G. W. Stuart, J-M. Kendall, and C. J. Ebinger (2005), Upper mantle seismic structure in a region of incipient continental breakup: Northern Ethiopian rift, *Geophys. J. Int.*, *162*, 479–493.

Berhe, S. M. (1990), Ophiolites in Northeast and East Africa: Implications for Proterozoic crustal growth, *J. Geol. Soc.*, *147*, 41–57.

Bilham, R., R. Bendick, K. Larson, P. Mohr, J. Braun, S. Tesfaye, and L. Asfaw (1999), Secular and tidal strain across the Main Ethiopian Rift, *Geophys. Res. Lett.*, *26*, 2789–2792.

Booth, D. C., and S. Crampin (1985), Shear-wave polarizations on a curved wavefront at an isotropic free-surface, *Geophys. J. R. Astron. Soc.*, *83*, 31–45.

Church, W. R., S. M. Berhe, M. G. Abdelsalam, and R. J. Stern (1991), Discussion of ophiolites in Northeast and East Africa: Implications for Proterozoic crustal growth, *J. Geol. Soc. London*, *148*, 600–606.

Crampin, S. (1994), The fracture criticality of crustal rocks, *Geophys. J. Int.*, *118*, 428–438.

do Nascimento, A. F., F. H. R. Bezerra, and M. K. Takeya (2004), Ductile Precambrian fabric control of seismic anisotropy in the Açu dam area, northeastern Brazil, *J. Geophys. Res.*, *109*, B10311, doi:10.1029/2004JB003120.

Ebinger, C., and M. Casey (2001), Continental breakup in magmatic provinces: An Ethiopian example, *Geology*, *29*, 527–530.

Evans, J. R., G. R. Foulger, B. R. Julian, and A. D. Miller (1996), Crustal shear-wave splitting from local earthquakes in the Hengill triple junction, southwest Iceland, *Geophys. Res. Lett.*, *23*, 455–458.

Kazmin, V., A. Shifferaw, and T. Balcha (1978), The Ethiopian basement: Stratigraphy and possible manner of evolution, *Geol. Rundsch.*, *67*, 531–546.

Kendall, J-M., G. W. Stuart, C. J. Ebinger, I. D. Bastow, and D. Keir (2005a), Magma assisted rifting in Ethiopia, *Nature*, *433*, 146–148.

Kendall, J-M., S. Pilidou, D. Keir, I. D. Bastow, A. Ayele, and G. W. Stuart (2005b), Mantle upwellings, melt migration and the rifting of Africa: Insights from seismic anisotropy, in *Structure and Evolution of the East African Rift in the Afar Volcanic Province*, edited by G. Yirgu, C. Ebinger, and P. Maguire, *Geol. Soc. Spec. Publ.*, in press.

Keranen, K., S. L. Klemperer, R. Gloaguen, and EAGLE Working Group (2004), Three-dimensional seismic imaging of a protoridge axis in the Main Ethiopian rift, *Geology*, *32*, 949–952.

Mackenzie, G. H., H. Thybo, and P. Maguire (2005), Crustal velocity structure across the Main Ethiopian Rift: Results from 2–dimensional wide-angle seismic modelling, *Geophys. J. Int.*, *162*, 994–1006.

Menke, W., B. Brandsdottir, S. Jakobsdottir, and R. Stefansson (1994), Seismic anisotropy in the crust at the mid-Atlantic plate boundary in south-west Iceland, *Geophys. J. Int.*, *119*, 783–790.

Miller, V., and M. Savage (2001), Changes in seismic anisotropy after volcanic eruptions: Evidence from Mount Ruapehu, *Science*, *293*, 2231–2233.

Silver, P. G. (1996), Seismic anisotropy beneath the continents, *Annu. Rev. Earth Planet. Sci.*, *24*(385), 432.

Silver, P. G., and W. W. Chan (1991), Shear-wave splitting and subcontinental mantle deformation, *J. Geophys. Res.*, *96*, 16,429–16,454.

Volti, T., and S. Crampin (2003), A four-year study of shear-wave splitting in Iceland: 2. Temporal changes before earthquakes and volcanic eruptions, in *New Insights Into Structural Interpretation and Modeling*, edited by D. A. Nieuwland, *Geol. Soc. Spec. Publ.*, *212*, 135–149.

Whaler, K. A., and S. Hautot (2005), The electrical resistivity structure of the crust beneath the northern Ethiopian rift, in *Structure and Evolution of the East African Rift in Afar Volcanic Province*, edited by G. Yirgu, C. Ebinger, and P. Maguire, *Geol. Soc. Spec. Publ.*, in press.

Wolfenden, E., C. Ebinger, G. Yirgu, A. Deino, and D. Ayalew (2004), Evolution of the northern Main Ethiopian rift: Birth of a triple junction, *Earth Planet. Sci. Lett.*, *224*, 213–228.

C. J. Ebinger and D. Keir, Department of Geology, Royal Holloway University of London, Egham TW20 0EX, UK. (d.keir@gl.rhul.ac.uk)

J-M. Kendall, Department of Earth Sciences, University of Bristol, Bristol BS8 1RJ, UK.

G. W. Stuart, School of Earth and Environment, University of Leeds, Leeds LS2 9JT, UK.